

Ab initio calculations of *f*-orbital electron-phonon interaction in laser cooling

Jedo Kim and Massoud Kaviani*

Department of Mechanical Engineering, University of Michigan, Ann Arbor, Michigan 48109-2125, USA

(Received 9 October 2008; revised manuscript received 15 December 2008; published 4 February 2009)

Results of *ab initio* calculation of electron-phonon interaction in laser cooling are reported and compared with the values estimated using analytical harmonic potential approximation. Electronic band-structure changes due to normal-mode ligand displacement are used to find the energy change in *f*-orbital optically active electron at the gamma point. The band-structure calculations show that the partial band structure of Yb is flat, indicating limited interaction with the neighboring atoms. The electron-phonon interaction potential calculated is within a factor 2 (larger) of the value using the harmonic potentials and the difference is attributed to the necessary approximations of each method. Single ligand displacement, which simulates one-phonon propagation, is also used and the resulting electron-phonon interaction potentials are in agreement with those from normal-mode vibration of the entire complex. Using these interaction potentials, larger cooling rates of the ion-host pair are calculated.

DOI: [10.1103/PhysRevB.79.054103](https://doi.org/10.1103/PhysRevB.79.054103)

PACS number(s): 31.15.A-, 78.20.Nv, 78.55.Hx, 71.20.-b

I. INTRODUCTION

In laser cooling of solid materials, many experimental and theoretical investigations have been carried out in the past decade to enhance the cooling performance. Experiments with rare-earth doped crystals have been successful in cooling to 208 K, from the room temperature.¹⁻³ Theoretical investigations focus on individual transition rates under assumed quantum models and have made significant progress.⁴⁻⁸ Still, very few experimental and theoretical studies have attempted to characterize the fundamental material properties involved in the interaction between the three carriers (photon, electron, and phonon) in laser cooling of solids.⁹ The challenge in the study of interaction carriers is that the existing theoretical investigations have been exclusively for semiconductors with band treatment of conduction electrons and they do not fully describe the carrier interaction for isolated ions. Especially the electron-optical phonon interaction is described by a normalization constant times deformation potential over the lattice constant. These values range up to tens of eV/Å for various semiconductor elements.¹⁰ However, in isolated rare-earth atoms, these defi-

nitions need to be modified and recent study shows that for rare-earth ions with insulator host, electron-phonon interaction potential was found to be significantly lower.⁷ In this study, we review the analytical harmonic approximation of the electron-phonon interaction potential made in Ref. 7, and compare it with *ab initio* calculations using isolated rare-earth host cluster and point out the validity of both methods and their limitations.

In anti-Stokes laser cooling of solids, the second-order process, where electron interacts with photon and phonon, for the cooling rate and the transition rate (using Fermi's golden rule) is^{11,12}

$$\dot{\gamma}_{\text{ph-e-p}} = \frac{2\pi}{\hbar} |M_{\text{ph-e-p}}|^2 \delta_D(E_{e,f} - E_{e,i} - \hbar\omega_{p,O}), \quad (1)$$

where $M_{\text{ph-e-p}}$ is the interaction matrix element of the photon, electron and phonon, δ_D is the Dirac delta function, $E_{e,f}$ and $E_{e,i}$ are the final and initial electronic energies, and $\omega_{p,O}$ is the phonon frequency involved in the process. Here $M_{\text{ph-e-p}}$ is expanded using second-order perturbation theory and is given as

$$M_{\text{ph-e-p}} = \sum_m \frac{\langle f | H_{\text{int}} | m \rangle \langle m | H_{\text{int}} | i \rangle}{E_{e,i} - E_{e,m}} \simeq \sum_m \frac{\langle \psi_f, f_{\text{ph}}, f_p | H_{\text{ph-e}} | \psi_m, f_{\text{ph}} + 1, f_p \rangle \langle \psi_m, f_{\text{ph}} + 1, f_p | H_{e-p} | \psi_i, f_{\text{ph}} + 1, f_p + 1 \rangle}{E_i - (E_m - \hbar\omega_p)}, \quad (2)$$

where subscript m designates intermediate states subsequent to phonon absorption but prior to photon absorption. With the interaction Hamiltonian for photon-electron and optical phonon-electron, the transition rate becomes

$$\dot{\gamma}_{\text{ph-e-p}} = \frac{\pi\hbar}{2m_{AC}} \frac{(s_{\text{ph},i} \cdot \boldsymbol{\mu}_{\text{ph-e}})^2}{\epsilon_0} \varphi_{e-p,O}^{i,2} \frac{D_p(E_p) f_p^0(E_p) \hbar\omega_{\text{ph},i} D_{\text{ph}}}{E_p^3 V}, \quad (3)$$

where m_{AC} is the reduced mass of the oscillating pair, $\mathbf{s}_{\text{ph},i}$ is photon polarization vector, $\boldsymbol{\mu}_{\text{ph}-e}$ is transition dipole moment vector, $\varphi'_{e-p,O}$ is electron-phonon interaction potential when optical phonon interaction is assumed, $D_p(E_p)$ is density of states of phonons having energy E_p , f_p is Bose-Einstein distribution function, $\omega_{\text{ph},i}$ is incoming photon frequency, and D_{ph} is the photon density of states which integrates to unity, since the incoming laser light is assumed to be monochromatic (and one-photon interaction is assumed).

In rare-earth ions, the f electron shell is optically active and when placed in a crystal-field environment, the electron energy levels split. Particularly for Yb^{3+} , due to the large spin-orbit coupling, ${}^2F_{5/2}$ is approximately $10\,000\text{ cm}^{-1}$ ($\approx 1.2\text{ eV}$) above ground state ${}^2F_{7/2}$. The crystal-field interaction further splits the excited and the ground-state electron energy levels depending on the ligand environment. This energy splitting is within a few $k_B T$ (comparable to phonon energy) and makes the anti-Stokes cooling possible. The electronic energy levels of the shell move up and down at finite temperature, because of the continuous excitation and de-excitation from phonon. Under the adiabatic approximation, the electron-phonon interaction is represented by

$$-\frac{\hbar^2}{m_e} \frac{\partial \Psi(Q)}{\partial Q} \frac{\partial \Phi_Q(r)}{\partial Q} = H_{e-p} \Psi(Q) \Phi_Q(r), \quad (4)$$

where m_e is the electron mass, $\Psi(Q)$ is the lattice wave function which depends on the normal coordinate Q , $\Phi_Q(r)$ is electronic wave function which depends on r which is the coordinate of the ion, and H_{e-p} is interaction Hamiltonian. We use a simple model developed in Ref. 13 to model the interaction. As mentioned above, the ion continuously moves due to lattice vibration and this movement changes the potential in the lattice. This change in the potential is experienced as a perturbation for the electron and scatters it to other electronic states and the energy change can be written as

$$\Delta E_{e-p} \equiv \sum_i \Delta_{p,i} \frac{\partial \varphi_{e-p,O}}{\partial \Delta_p}, \quad (5)$$

where ΔE_{e-p} is the energy change in the electron due to phonon (lattice vibration), Δ_p is the displacement of the atom, and $\varphi_{e-p,O}$ is the potential change due to the perturbation which is called the electron-phonon coupling.

In Yb^{3+} the electronic energy level oscillations by phonon take place within the energy level splitting due to crystal-field interaction at ground or excited energy levels. In laser cooling of solid using rare-earth ions, optically active $4f$ electronic shells (partial electronic energy change) are significant. The energy change is found by comparing the electronic band structure of the equilibrium cluster with nonequilibrium (displaced). Here we do this for ground state $4f$ orbital of Yb at the Γ point.

Figure 1 shows a conceptual (model) rendering of the electronic energy change in ion-ligand complex under ligand displacement. The partial electronic band structure of Yb in host (Yb electron interaction with potential created by the neighboring ligands) is also shown. In Ref. 7, a simplified harmonic potential is used between atoms and estimates of

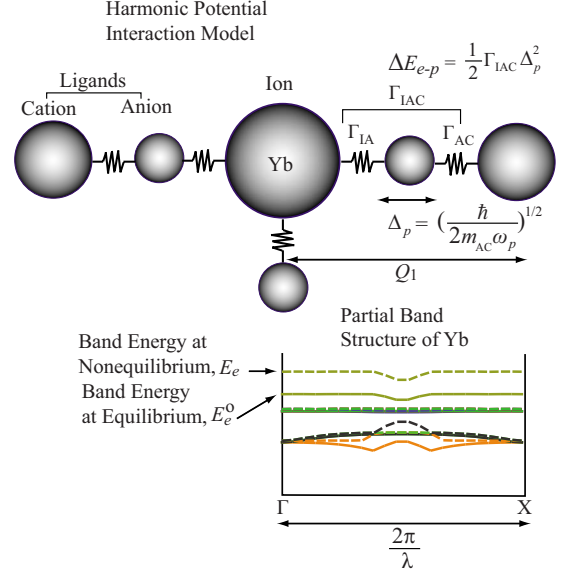


FIG. 1. (Color online) A conceptual rendering of the ion-ligand complex under atomic displacement due to phonon excitation. The energy change in the electron using harmonic potential can be represented by the equivalent potential energy change in the complex. *Ab initio* calculations show the change in the partial electronic band structure of the ion at the Γ point due to atomic displacement. The equilibrium and displaced band structures are indicated by solid and broken lines, respectively, and the corresponding electronic energies are marked on y axis (E_e^0 is for the equilibrium and E_e is for the displaced).

the electron-phonon interaction potential for rare-earth materials are made. It uses experiential results for force constants for mononuclear pair atoms and the combinative rule to extrapolate the force constants between different atoms. This gives

$$\Gamma_{IAC} = [(\Gamma_{AA}\Gamma_{CC})^{1/2}\Gamma_{II}]^{1/2}, \quad (6)$$

where Γ_{AA} , Γ_{CC} , and Γ_{II} are the force constants of the anion-anion, cation-cation, and ion-ion, respectively.

The atomic displacement is found by using the stretching-mode amplitude of the ligand pair (cation and anion) by a quantum of the most probable phonon energy and this is given by

$$\Delta_p = \left(\frac{\hbar}{2m_{AC}\omega_p} \right)^{1/2}, \quad (7)$$

where Δ_p is the amplitude of displacement, m_{AC} is the reduced mass of the anion and cation, and ω_p is the angular frequency of the phonon. Then assuming that the optically active electron of the ion is in an infinite square well, we estimate the energy change in the electron using appropriate boundary conditions. The potential change between the atoms under ligand displacement and the corresponding interaction potential are given by (also shown in Fig. 1)

TABLE I. Lattice constants used in the *ab initio* calculations and their relaxed values. The displacements of the ligands are also shown (Refs. 14 and 15).

Compound and structure	Symmetry	Q_1^o (Å)	Q_1 (Å)	Δ_p (Å)
Yb: CdF ₂ (cubic)	<i>Fm</i> 3 <i>m</i>	3.786	3.862	0.068
Yb: CaF ₂ (cubic)	<i>Fm</i> 3 <i>m</i>	3.861	3.938	0.082
Yb: MgF ₂ (tetragonal)	<i>m</i> 3 <i>m</i>	3.605	3.695	0.089

$$\Delta E_{e-p} = \frac{1}{2} \Gamma_{IAC} \Delta_p^2, \quad \varphi'_{e-p,O} \equiv \frac{\Delta E_{e-p}}{Q_1}, \quad (8)$$

where Q_1 is the distance between the ion and closest cation. Despite its simplicity, the harmonic potential estimate of the electron-phonon interaction gives reasonable estimates and is used in laser cooling of solids.⁷ To further verify the validity of this model, below we perform *ab initio* calculations using Yb ion in various hosts to determine the electron-phonon interaction potential.

II. CALCULATION

The calculation of the electronic energy change due to ligand displacement is performed using WIEN2K which is based on the full potential (linearized) augmented plane-wave (L)APW and local orbital method. (L)APW method is considered as one among the most accurate schemes for band-structure calculations. A $2 \times 2 \times 2$ supercell is first created then the ligands are removed until irreducible unit cell is created. The supercell and the irreducible unit cell are shown in Fig. 1. Then the central cation atom is replaced by the Yb ion to simulate doping. Then using WIEN2K, the whole structure is relaxed until equilibrium is reached. Table I. shows the structure, symmetry, Q_1^o of bulk, Q_1 of relaxed structure and corresponding ligand displacements for the compounds used in the *ab initio* calculations. At this equilibrium geometry, the partial band structure of the Yb atom is calculated and compared with a displaced structure, where ligand displacement is simulated by displacement of the immediate neighboring atoms (Fig. 2). The band-structure calculation is carried out until energy convergence of 0.002 Ry is reached.

III. RESULTS AND DISCUSSION

Figure 3 shows the band structure of CdF₂ and the partial band structures of Yb 4*f* orbital are shown by broken lines for both equilibrium structure and the displaced structure (all the immediate ligands were displaced radially outward to simulate the normal-mode vibration) as shown in Fig. 2(b). Only the band structure near the Fermi energy is shown and the partial band structures of Yb 4*f* orbital all lie between the shown energy interval. The displacement magnitude was calculated using Eq. (7) with phonon energy distributed among all the neighboring eight sets of ligands. The discrete energy levels resemble isolated ions which indicates that the Yb ion remains as an impurity. The band structure of 4*f* orbital is generally flat, indication limited interaction with neighboring

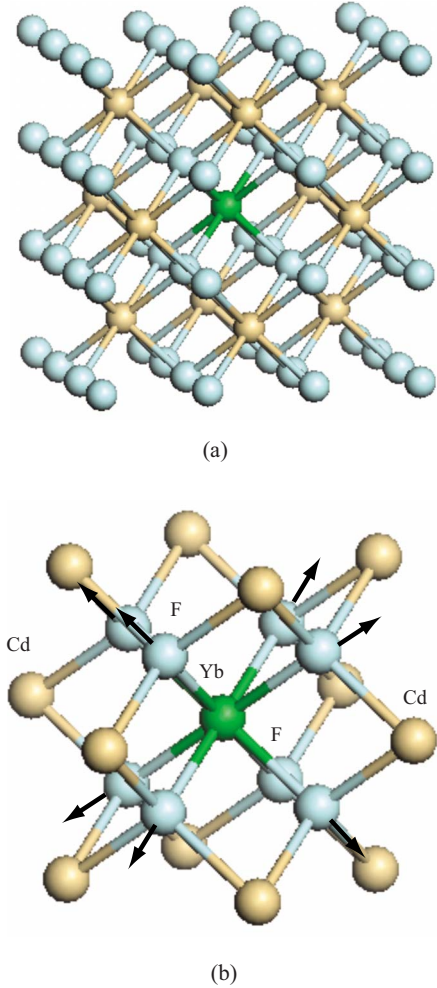


FIG. 2. (Color online) (a) shows the $2 \times 2 \times 2$ supercell created for doping of Yb atom in CdF₂ host. (b) shows the Yb: CdF₂ complex constructed by removing outer ligands which is not expected to influence 4*f* electron shell of Yb. The simulated ligand movement is also shown by arrows pointing away from the central ion.

potentials although slight curvatures are present. Also, the electronic energy levels are close to the Fermi level, making them available for optical interactions. From the partial electron band, we select the band which has highest energy (outmost electron level) which is also closest to the Fermi level. At the Γ point, the corresponding electronic band energy is designated by E_e^o . The electronic band structure of the non-equilibrium structure indicates a shift in energy from the equilibrium structure and is designated by E_e . Then the change in the outmost electron energy level and the corresponding electron-phonon interaction potential becomes

$$\Delta E_{e-p} = E_e - E_e^o, \quad \varphi'_{e-p,O} \equiv \frac{E_e - E_e^o}{Q_1}. \quad (9)$$

Using this definition, we calculate the energy change in the 4*f* electron shell of the ground state Yb due to longitudinal ligand displacement (normal-mode displacement). Table II compares the calculated values with the approximated values using the force constants for different host materials and the

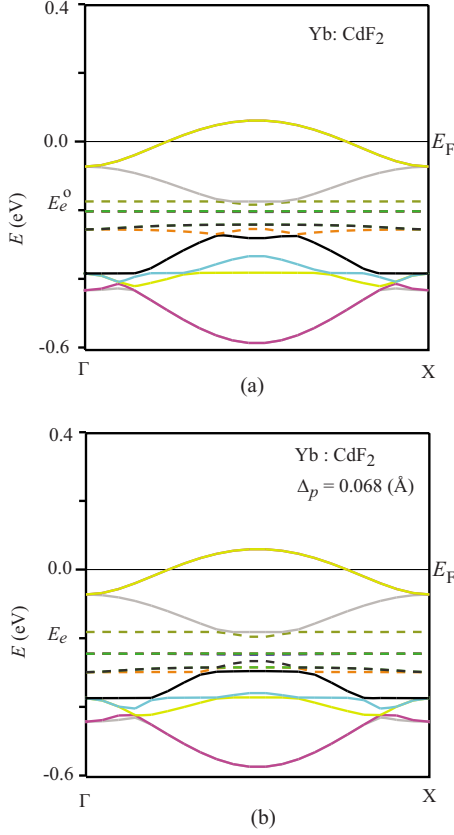


FIG. 3. (Color online) Electronic band structure of CdF_2 doped with Yb. The strongest partial electronic band structures of Yb are shown by broken lines. (a) shows the equilibrium structure, and (b) shows the nonequilibrium structure with the breathing mode displacement.

corresponding Fermi energies are also given. The results are found to be in good agreement for the electron-phonon interaction potential calculated using the force constants in Ref. 7. Note that both methods employ approximations in calculating the electron-phonon interaction potential. The pair harmonic approximation uses one ligand interaction model where the potential is not affected by other ligands. Thus, it is expected to underestimate $\varphi'_{e-p,O}$. Also, the geometry of the ion-ligand complex is simplified, where in a real crystal, the geometry can be quite complex. On the other hand, the *ab initio* calculation is expected to overestimate the interaction potential, since it is very difficult to separate the band struc-

TABLE II. Comparison of the electron-phonon interaction potential between estimates based on harmonic potentials and values calculated using *ab initio* methods.

Compound	Fermi energy (eV)	Harmonic approximation $\varphi'_{e-p,Q}$ (eV/Å)	<i>Ab initio</i> calculation $\varphi'_{e-p,Q}$ (eV/Å)
Yb: CdF ₂	-0.150	0.00152	0.00232
Yb: CaF ₂	-0.153	0.00182	0.00289
Yb: MgF ₂	-0.244	0.00222	0.00355

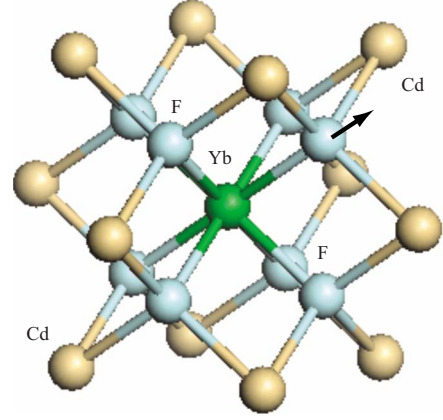


FIG. 4. (Color online) One ligand displacement of the Yb: CdF₂ complex, which simulates one quantum of longitudinal phonon propagation.

ture of the optically active ion from the core electrons. Also, the supercell is created from an electrostatically neutral anion-cation pair, which does not represent the real charge distribution for Yb^{3+} in host crystal. Nevertheless, the comparison in Table I shows that estimations of $\varphi'_{e-p,O}$ using the two methods are in reasonable agreement.

Further calculations are carried out by simulating single ligand movement, which can be interpreted as one quantum of longitudinal optical phonon propagating through the ion-ligand complex of Yb: CdF₂, as shown in Fig. 4. For single-ligand displacement, $\Delta_p = 0.194$ Å is used and the corresponding $\varphi'_{e-p,O}$ was found to be 0.00257 eV/Å, which is very close to the value obtained using the normal-mode vibration of the entire complex. This slightly larger value is believed to be attributed to the anharmonic effects, because of the relatively large displacement amplitude.

We use the above $\varphi'_{e-p,O}$ for the normal-mode vibration to calculate the normalized cooling rate of $\text{Yb}^{3+}:\text{Cd-F}$ and compare it with the rate calculated using the harmonic potential approximation. The normalized cooling rate is¹¹

$$\frac{\dot{S}_{\text{ph-e-p}}}{Q_{\text{ph},i}} = n_d V \tau_{\text{ph,tr}} \dot{\gamma}_{\text{ph-e-p}} \left(1 - \frac{\bar{\omega}_{\text{ph},e}}{\omega_{\text{ph},i}} \eta_{\text{ph-e}} \right), \quad (10)$$

where $Q_{\text{ph},i}$ is the input laser irradiation power, n_d is the number of dopants, V is the volume, $\tau_{\text{ph,tr}}$ is the photon transit time of light along the length of the sample (assuming a single pass), $\dot{\gamma}_{\text{ph-e-p}}$ is the phonon-assisted, phonon absorption rate given by Eq. (3), $\omega_{\text{ph},e}$ and $\omega_{\text{ph},i}$ are absorbed and emitted photon frequencies, respectively, and $\eta_{\text{ph-e}}$ is the quantum efficiency given as a ratio of radiative decay rate with respect to the radiative decay rate plus nonradiative decay rate [$\dot{\gamma}_{\text{ph-e}} / (\dot{\gamma}_{\text{ph-e}} + \dot{\gamma}_{e-p})$]. Figure 5(a) shows the variations in normalized cooling rate with respect to absorbed phonon energy for $\text{Yb}^{3+}:\text{Cd-F}$.

The results show that at $E_p = 0.032$ eV, when the incoming photon wavelength is equal to average emission wavelength ($\omega_{\text{ph},i} = \bar{\omega}_{\text{ph},e}$), the net cooling effect is zero. As the energy of the absorbed phonon decreases, heating occurs (indicated by positive value of $\dot{S}_{\text{ph-e-p}} / Q_{\text{ph},i}$). As the energy of

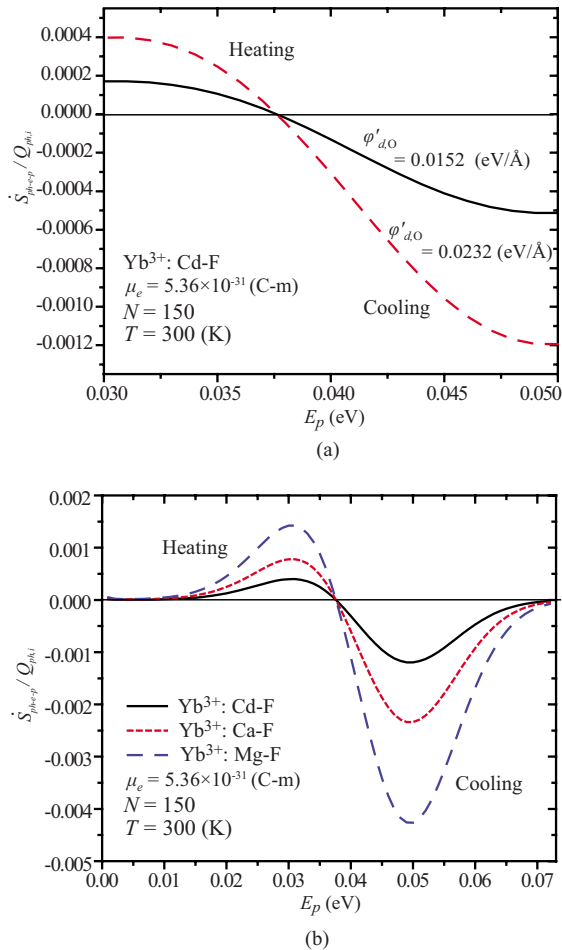


FIG. 5. (Color online) (a) Variations in the normalized cooling rate of $\text{Yb}^{3+}:\text{Cd-F}$ with respect to absorbed phonon energy (variance in input photon energy). Broken line with higher $\phi'_{e-p,O}$ value found from *ab initio* calculations and solid line with lower $\phi'_{e-p,O}$ value found from the harmonic potential. (b) Variations in the normalized cooling rate of $\text{Yb}^{3+}:\text{Cd-F}$, Ca-F and Mg-F with respect to absorbed phonon energy (variance in input photon energy). N is the number of atoms near the ion which contributes to the phonon modes.

the absorbed phonon increases, cooling occurs and reaches a plateau at approximately $\hbar\omega_p = 0.045$ eV. For both heating and cooling, the rates calculated using the *ab initio* $\phi'_{e-p,O}$ are higher. Figure 5(b) shows the variation in normalized cooling rate with respect to absorbed phonon energy for Yb^{3+} ion in three different host crystals (Cd-F, Ca-F, and Mg-F). The result shows that higher $\phi'_{e-p,O}$ is favored in optimizing the cooling rates; i.e., more Mg-F should be used rather than Cd-F. However, as one increases the concentration of Mg-F, probability of parasitic heating increases when reabsorption is present. Therefore, in material metrics for laser cooling of solids, there always exists a competition between heating and cooling, as the interaction strengths of the carriers change. Further investigations should include the excited-state electron-phonon interaction potential, which helps in understanding the phonon interactions in optical transition processes

IV. CONCLUSION

The electron-phonon interaction potential is central in understanding or optimizing the phonon (thermal) effects in laser cooling (optical transition process). Here, we have performed *ab initio* calculations of this interaction potential by calculating the partial electronic energy change due to the imposed ligand displacement. It was found that the calculated value overestimates the value previously using harmonic potentials between the atoms. However, these differences result in different simplifying approximations needed in each model. Normalized cooling rates are found using both the *ab initio* calculated and the harmonic potential estimated values of the electron-phonon interaction potential. The results show that the higher the interaction strength, the higher the cooling and heating rates.

ACKNOWLEDGMENTS

The support through NSF Grant No. CTS-0553651 is greatly appreciated. We are thankful to Xiulin Ruan, Baoling Huang, and the WIEN2K mailing group for their valuable discussions and suggestions.

*kaviany@umich.edu

¹T. R. Gosnell, Opt. Lett. **24**, 1041 (1999).

²J. Fernandez, A. J. Garcia-Adeva, and R. Balda, Phys. Rev. Lett. **97**, 033001 (2006).

³J. Thiede, J. Distel, S. R. Greenfield, and R. I. Epstein, Appl. Phys. Lett. **86**, 154107 (2005).

⁴X. L. Ruan and M. Kaviany, Phys. Rev. B **73**, 155422 (2006).

⁵M. P. Hehlen, R. I. Epstein, and H. Inoue, Phys. Rev. B **75**, 144302 (2007).

⁶D. Emin, Phys. Rev. B **76**, 024301 (2007).

⁷J. Kim, A. Kapoor, and M. Kaviany, Phys. Rev. B **77**, 115127 (2008).

⁸H. Bao, X. L. Ruan, and M. Kaviany, Phys. Rev. B **78**, 125417

(2008).

⁹X. L. Ruan and M. Kaviany, J. Comput. Theor. Nanosci. **5**, 221 (2008).

¹⁰W. Pötz and P. Vogl, Phys. Rev. B **24**, 2025 (1981).

¹¹M. Kaviany, *Heat Transfer Physics* (Cambridge University Press, New York, 2008).

¹²R. C. Powell, *Physics of Solid-State Laser Material* (Springer-Verlag, New York, 1998).

¹³J. M. Ziman, *Electrons and Phonons* (Oxford University Press, London, 1962).

¹⁴J. P. Poirier, Phys. Earth Planet. Inter. **31**, 187 (1983).

¹⁵D. N. Batchelder and R. O. Simmons, J. Chem. Phys. **41**, 2324 (1964).